

Supplementary information

Mechanically robust cationic cellulose nanofibril 3D scaffolds with tuneable biomimetic porosity for cell culture

James C. Courtenay, Jefferson G. Filgueris, Eduardo Riberio de Azevêdo, Yun Jin, Karen J. Edler, Ram I. Sharma and Janet L. Scott

Characterisation of modified cellulose:

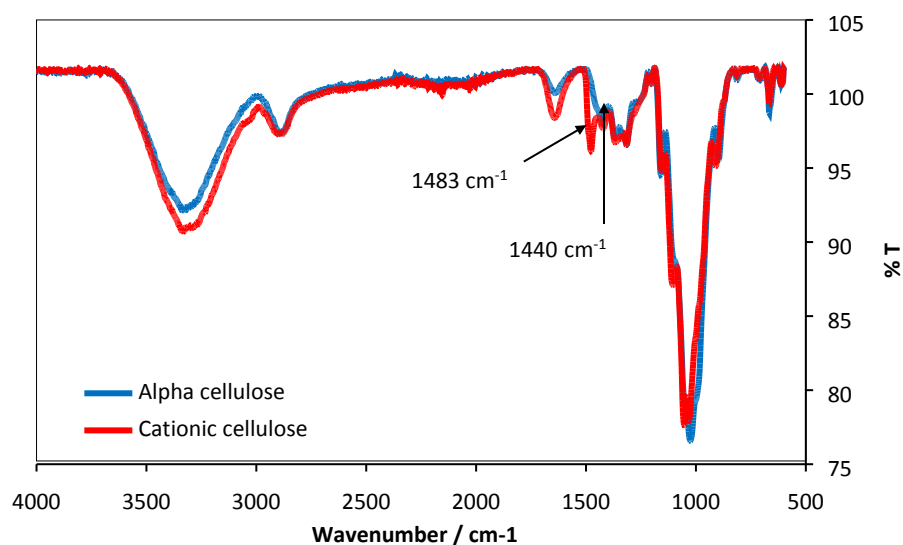


Fig. S1 FTIR spectra for unmodified α -cellulose and CCNF (DS = 23.0 ± 0.9 %) powders were obtained on a Perkin Elmer Spectrum 100 with a universal ATR sampling accessory; 10 scans were acquired in the range 4000 – 600 cm⁻¹. FTIR: prominent bands at 1440 cm⁻¹ and 1483 cm⁻¹ were attributed to the CH₂ bending mode and methyl groups of the cationic cellulose substituents in accordance with data published by Zaman *et al.*².

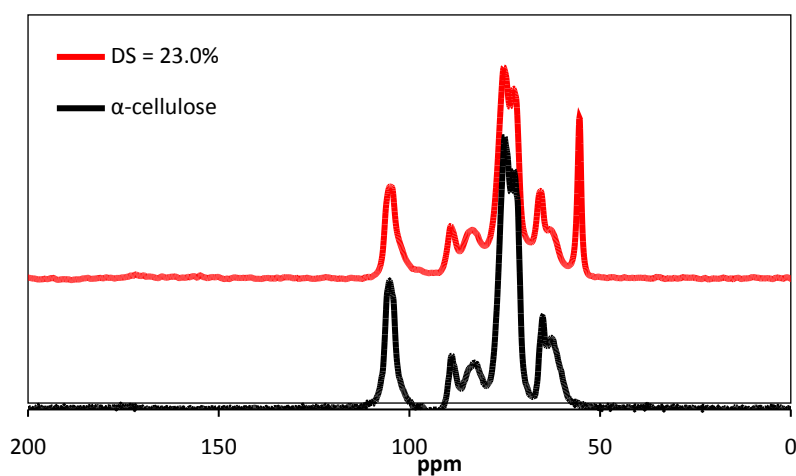


Fig. S2 ¹H-¹³C CP/MAS NMR spectra for α -cellulose and CCNF (DS = 23.0%) powders, acquired using MAS rates of 10 kHz. The signal at 55.5 ppm is assigned to the methyl carbon resonances of the quaternary ammonium group and used to determine DS.

Conductometric analysis of degree of substitution:

The degree of substitution of cationic cellulose was determined by conductometric titration of chloride ions (trimethylammonium chloride groups) with AgNO_3 (aq) as described previously.¹ The conductivity was monitored using a SevenMulti Mettler Toledo conductivity probe. The degree of substitution is calculated by:

$$\text{Degree of Substitution \%} = \left[\frac{162.15 \times (C \times V)}{w - (151.63 \times C \times V)} \right] 100 \quad (\text{Eqn. 1})$$

Where C is the concentration of AgNO_3 solution (M), V is the volume of AgNO_3 solution (in dm^3), and w is the weight of the dried cationised cellulose sample (g), 162.15 is the M_w of the anhydroglucose unit (AGU) and 151.63 is the difference in M_w between the AGU and cationised AGU bearing trimethylammonium chloride groups. Triplicate samples were analysed and an average reported.

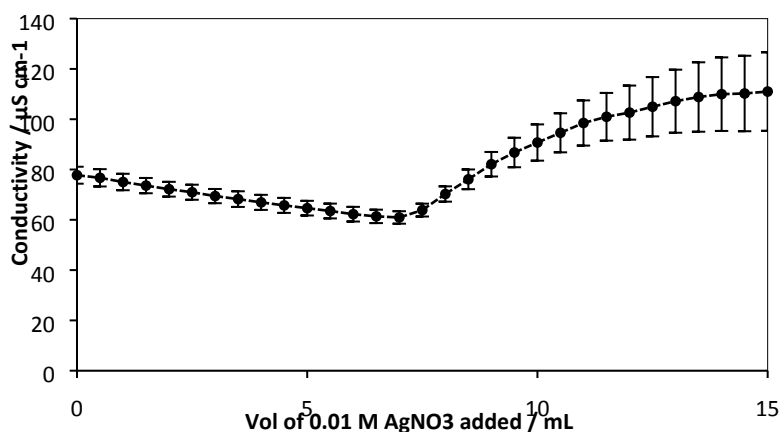


Fig. S3 Conductivity curve for CCNF in DI H_2O titrated with $ca \sim 1 \text{ mM}$ AgNO_3 in 0.50 mL aliquots.

Degree of crosslinking:

The degree of crosslinking (DXL) was determined by HPLC analysis following a method adapted from Schramm *et al.*³ Briefly, dry crosslinked cellulose films were hydrolysed, filtered, and the concentration of glycolic acid in each solution was determined by HPLC analysis. Once the mass of glyoxal present in the crosslinked films was determined (using a calibration curve) the DXL was calculated using the following equation:

$$\text{Degree of Crosslinking \%} = \left[\frac{162.15 \times \text{Mol}_{\text{glyoxal}}}{w - (58.04 \times \text{Mol}_{\text{cellulose}})} \right] 100 \quad (\text{Eqn. 2})$$

Where $\text{Mol}_{\text{glyoxal}}$ is the amount of glyoxal detected by HPLC (mol), $\text{Mol}_{\text{cellulose}}$ is the amount of crosslinked cellulose present (mol) and w is the weight of the dried crosslinked cellulose sample (g), 162.15 is the M_w of the AGU and 58.04 is the difference in M_w between the AGU and crosslinked AGU bearing a glyoxal group. Triplicate samples were analysed for each material and an average reported.

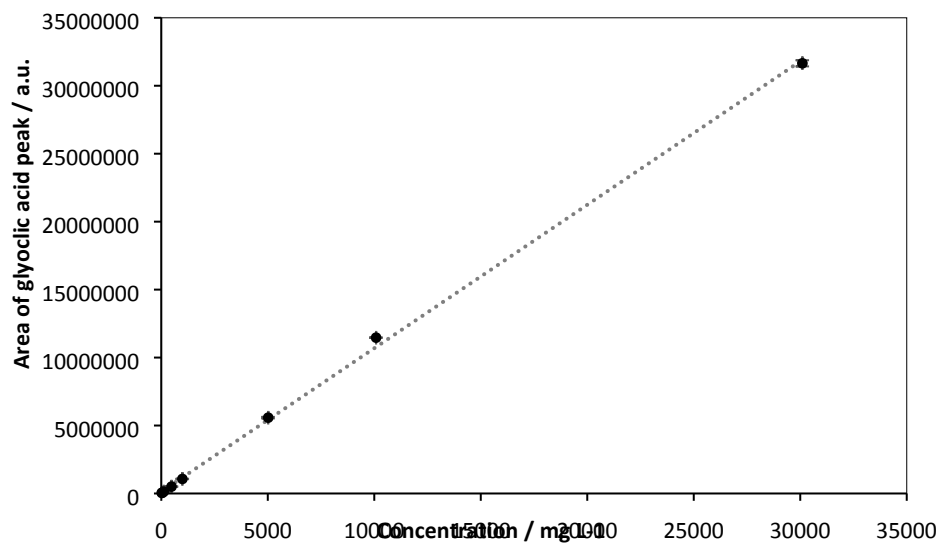


Fig. S4 Glycolic acid peak area for prepared standard solutions (20 – 30,000 mg L⁻¹). Calibration coefficient for glycolic acid was calculated from the gradient of the line to be 1055.5 a.u./ mg L⁻¹. (n = 3, error bars = standard deviation)

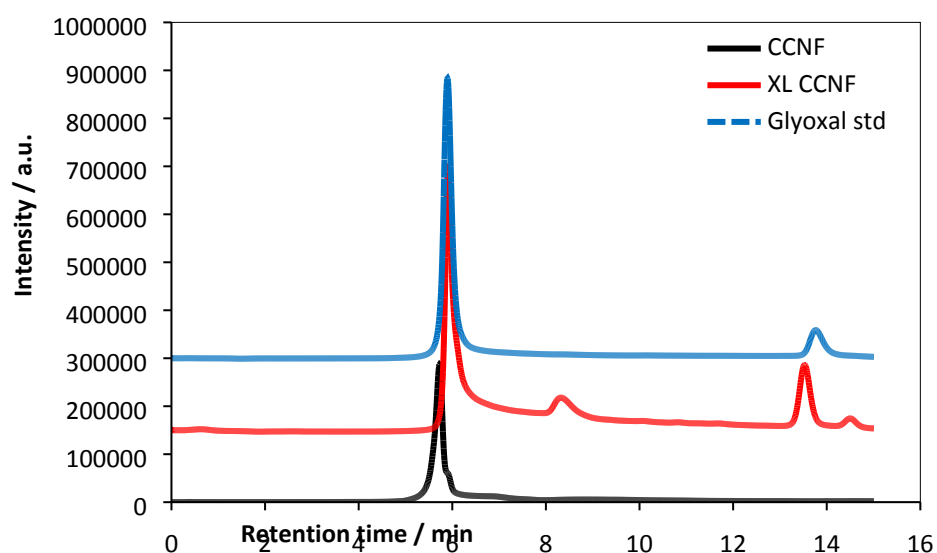


Fig. S5. HPLC analysis of glycolic acid present after the base hydrolysis of crosslinked cellulose foams. The large peak at 5.9 min refers to the solvent front and the peak for glycolic acid occurs at 13.7 min.

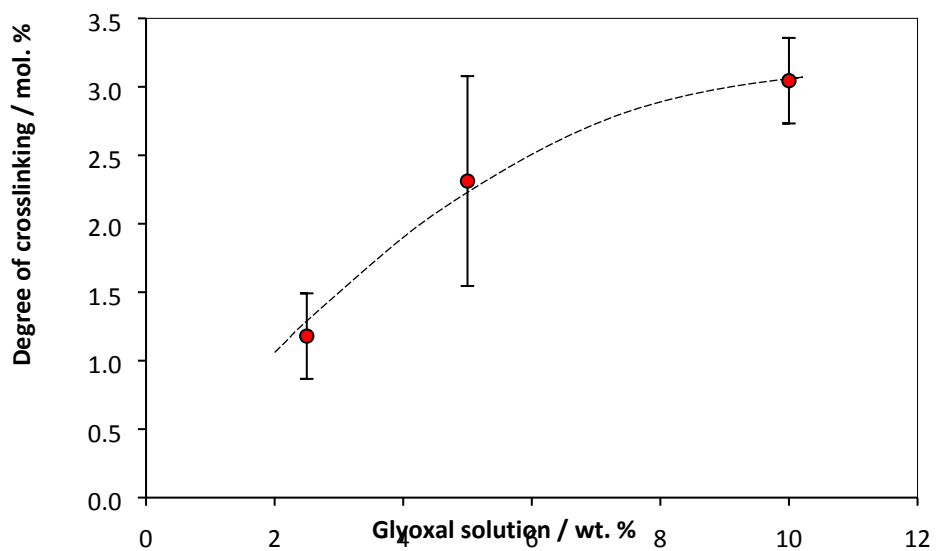


Fig. S6. The effect of glyoxal concentration on degree of crosslinking was calculated from the integrated area for the glycolic acid peak, which was proportional to the amount of glyoxal added to the CCNF dispersion (fitted line to guide the eye).

Formation of 3D scaffolds:

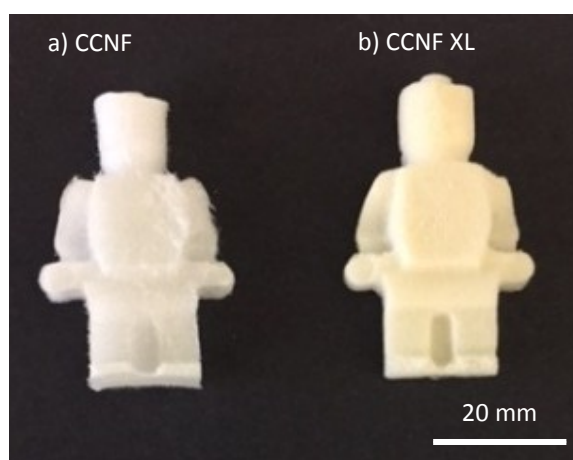


Fig. S7 Image of lyophilised 3D foam scaffolds produced from CCNF and CCNF XL hydrogels cast in moulds.

NMR Cryoporometry:

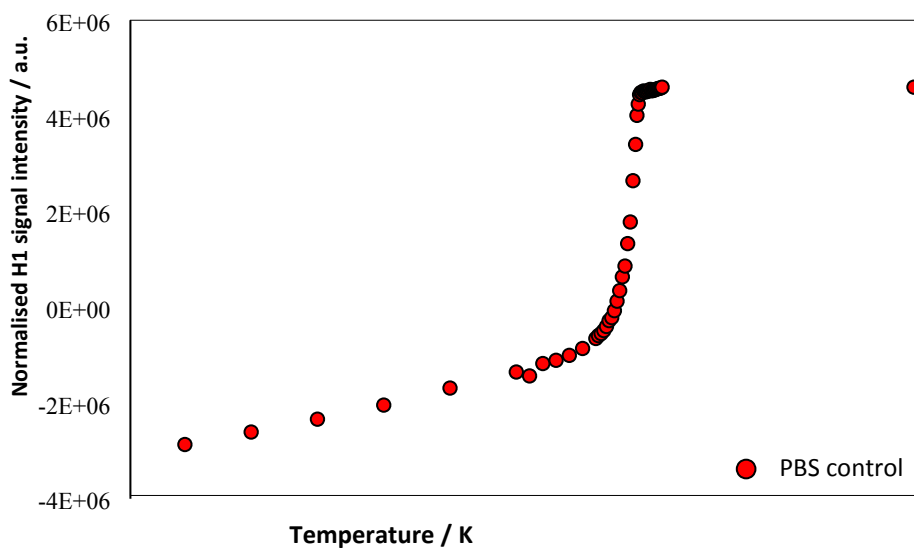


Fig. S8 H₂O signal peak intensity from H¹ NMR spectra from a PBS control in a temperature range from 218 K to 300 K.

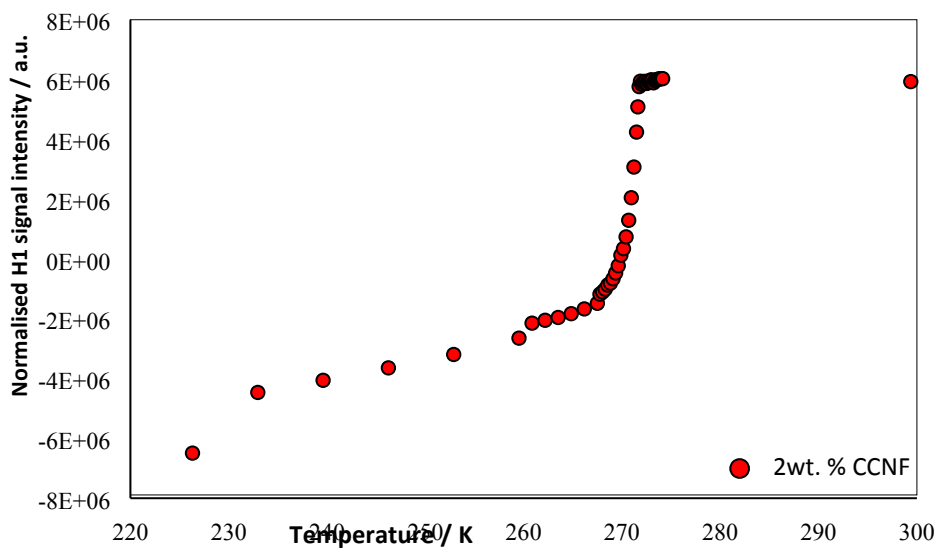


Fig. S9 H₂O signal peak intensity from H¹ NMR spectra from a hydrated CCNF sample in a temperature range from 218 K to 300 K

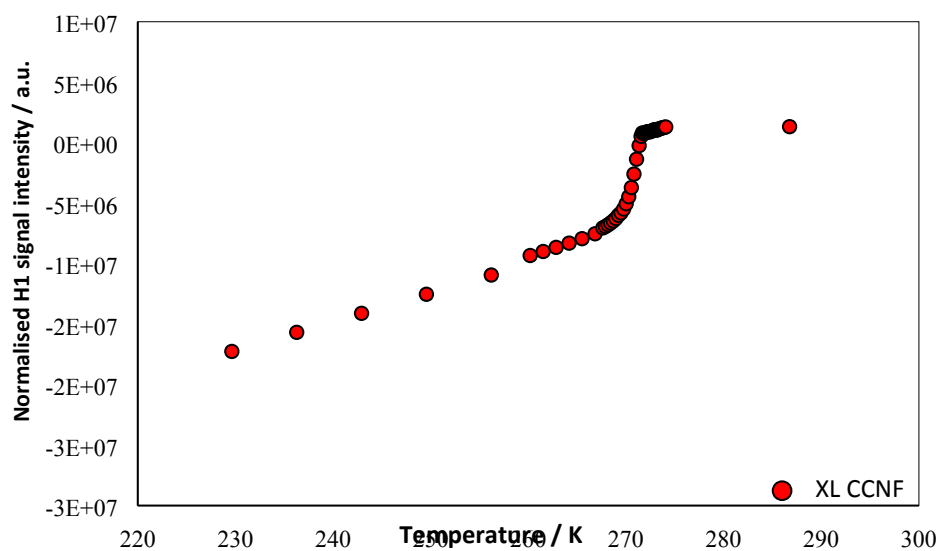


Fig. S10 H₂O signal peak intensity from H¹ NMR spectra from a hydrated CCNF XL sample in a temperature range from 218 K to 300 K

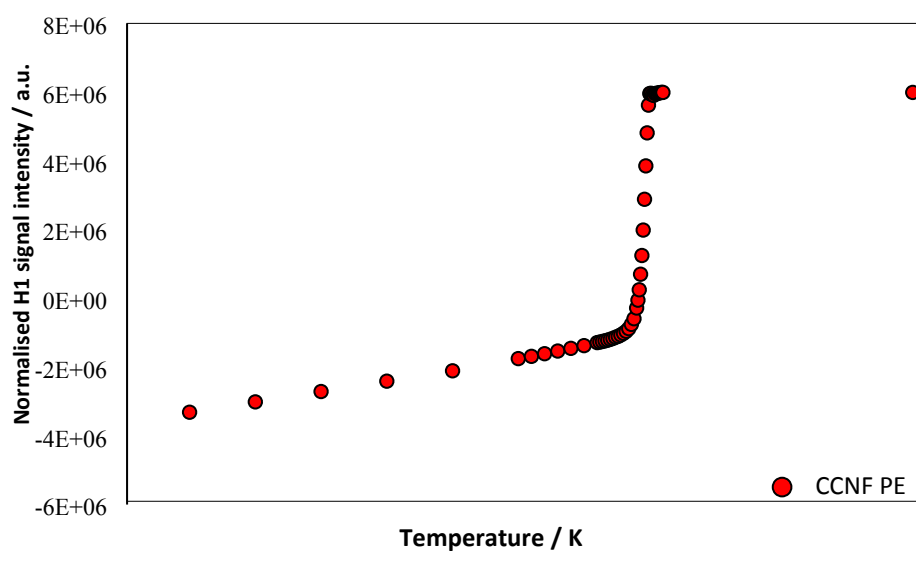


Fig. S11 H₂O signal peak intensity from H¹ NMR spectra from a hydrated CCNF PE sample in a temperature range from 218 K to 300 K

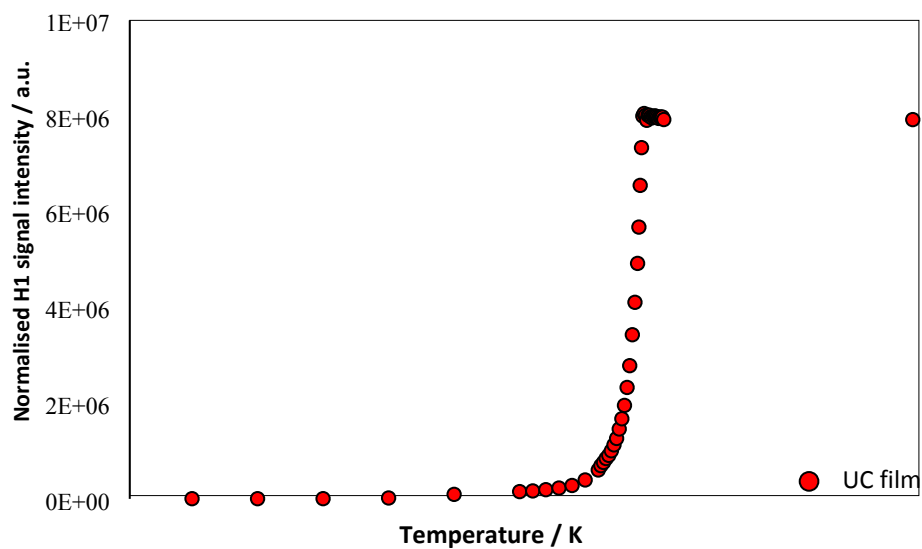


Fig. S12 H₂O signal peak intensity from H¹ NMR spectra from a hydrated UC film sample in a temperature range from 218 K to 300 K

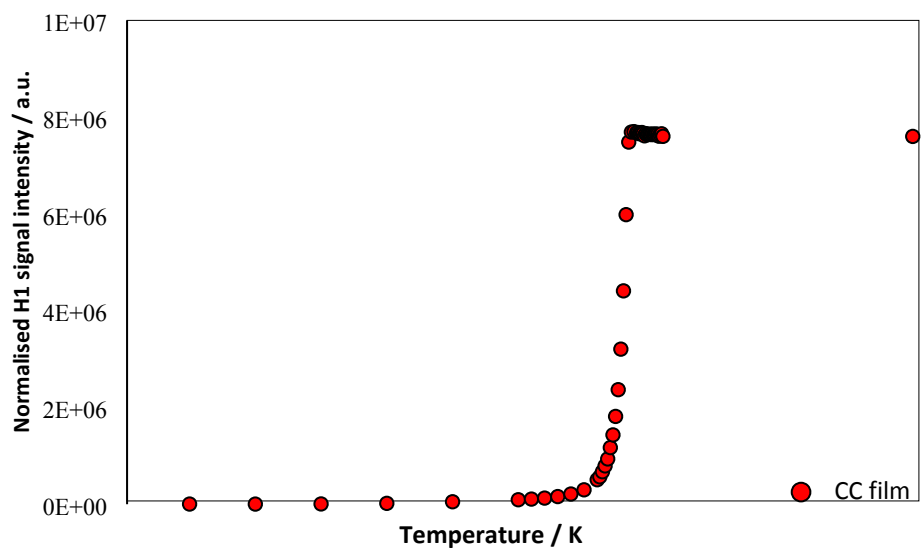


Fig. S13 H₂O signal peak intensity from H¹ NMR spectra from a hydrated CC film sample in a temperature range from 218 K to 300 K

T2 relaxometry:

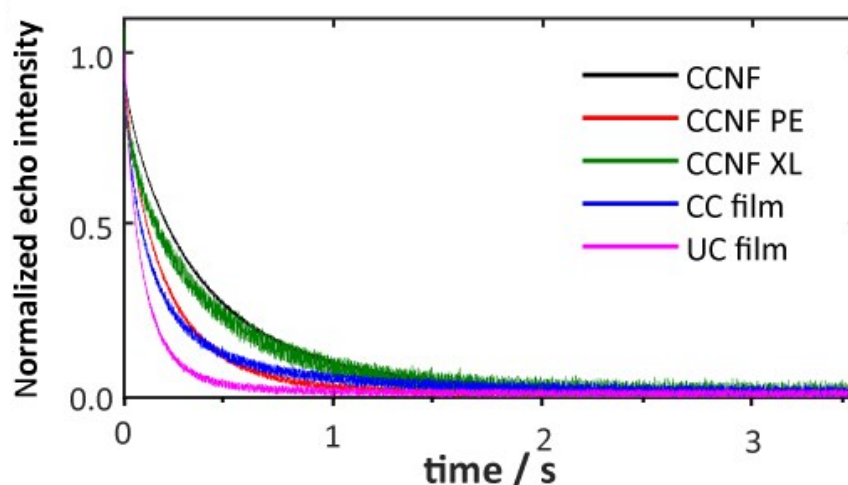


Fig. S14 Time decay of the echo intensities measured in Carr–Purcell Meiboom–Gill (CPMG) NMR experiments for all samples. The signal clearly shows different decay rates associated with distinct pore structures.

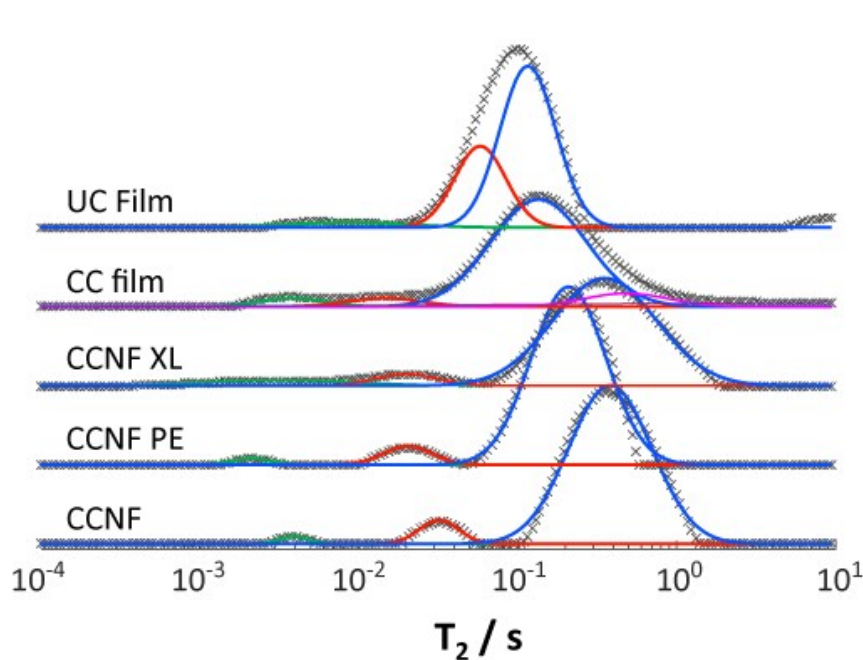


Fig. S15 The T_2 distributions for all samples, obtained from the ILT procedure^{4,5} applied to the CPMG decays and normalized by area. Three length scales are observed on the distributions: nanopores, ranging from 10^{-3} to 10^{-2} s, mesopores, from 10^{-2} up to 10^{-1} s and large pores, for T_2 from 10^{-1} s. The asymmetry of the large pore component for the CC film is due to the presence of free solvent in the sample, and is not considered in the analysis. (Free solvent refers to fluid contained in pores that are large enough not to affect the transverse relaxation.^{6,7})

Similar distributions for the three CCNF samples were observed with almost no overlap between the components. The UC and CC films have a significant difference on the mesopore scale, with a bigger relative area on the UC film. This means that there are more DMAc molecules, in proportion, on this scale on the UC film than in the CC material.

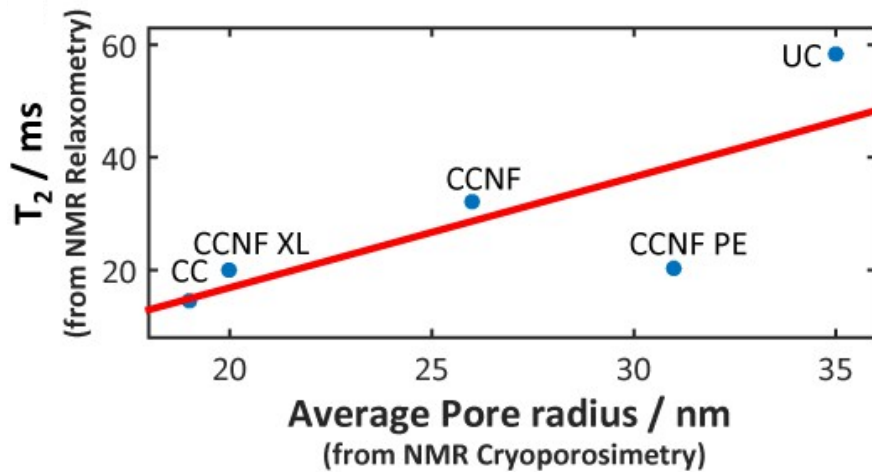


Fig. S16. Correlation between the mesopore components of the T_2 distributions above and the pore sizes estimated from cryoporometry measurements. The correlation coefficient between the two data sets is given by $R^2 = 0.77$.

Once this correlation was established, it provided the proportionally factor between T_2 and pore radius values, which allow estimation of the sizes of the larger pores (length scale of hundreds nanometers), from the NMR data, providing extra information about pore sizes on a length scale that neither NMR cryoporometry nor SEM could be used to probe.

SEM analysis:

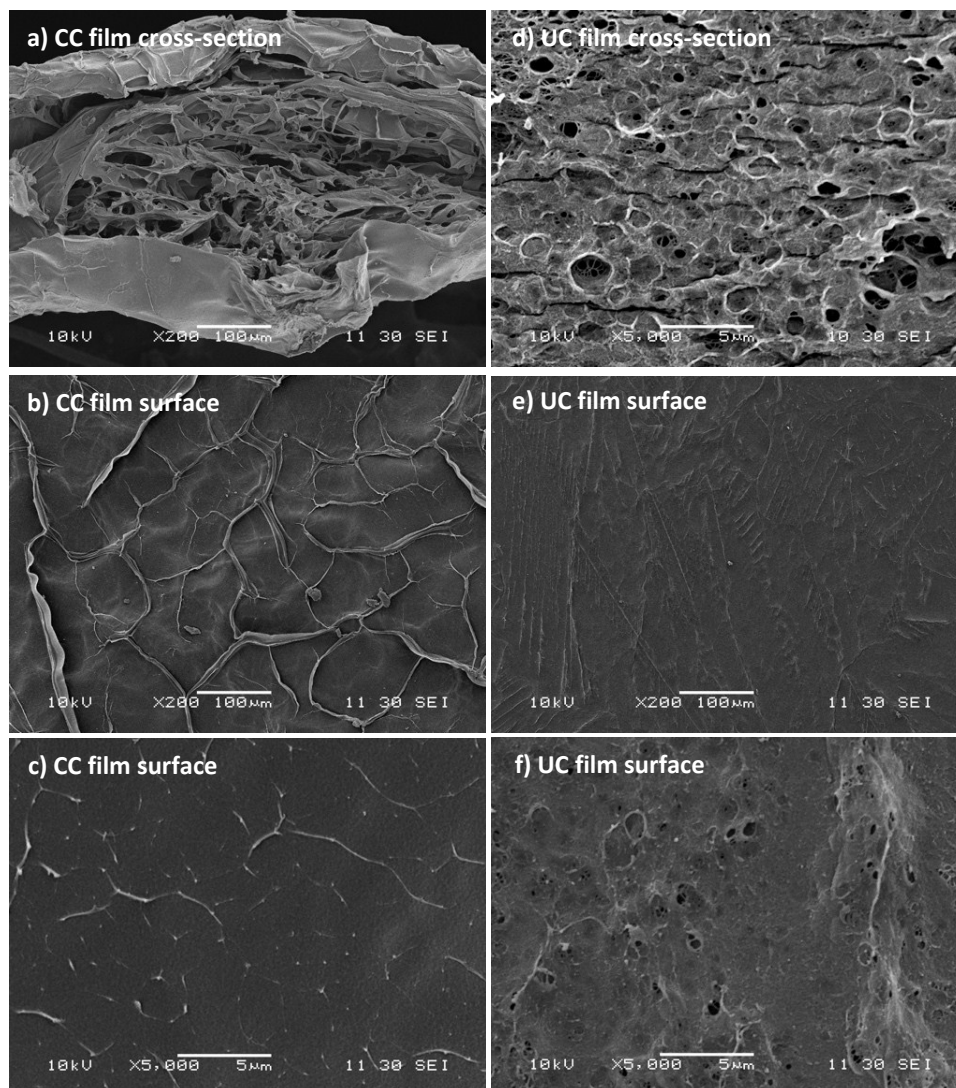


Fig. S17 SEM images of films: a, b and c) lyophilised, regenerated CC and d, e and f) unmodified cellulose. The porosity in the films is evident in the images of film cross-sections (a and d), but not at the surface. A “skin” on the surface of the films is due to the anti-solvent regeneration process.

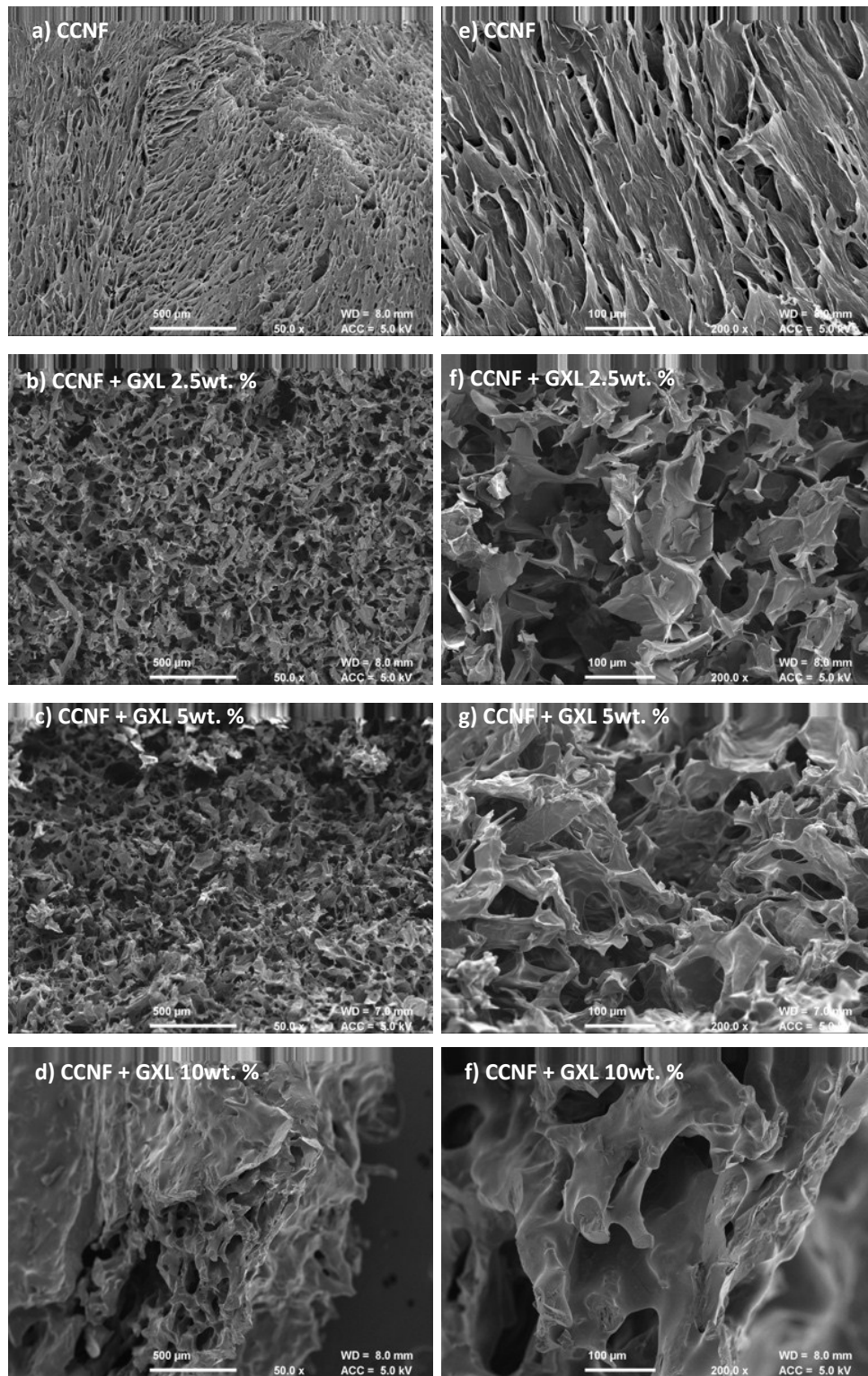


Fig. S18 SEM images of lyophilised CCNF foams; a) CCNF, b) CCNF + 2.5 wt. % glyoxal, c) CCNF 5 wt. % glyoxal and d) CCNF 10 wt. % glyoxal, and at higher magnification e) CCNF, f) CCNF + 2.5 wt. % glyoxal, g) CCNF 5 wt. % glyoxal and h) CCNF 10 wt. % glyoxal. ImageJ software was used to analyse the images to characterise porosity. It is apparent that the amount of glyoxal present in the hydrogel affected the pore size and morphology.

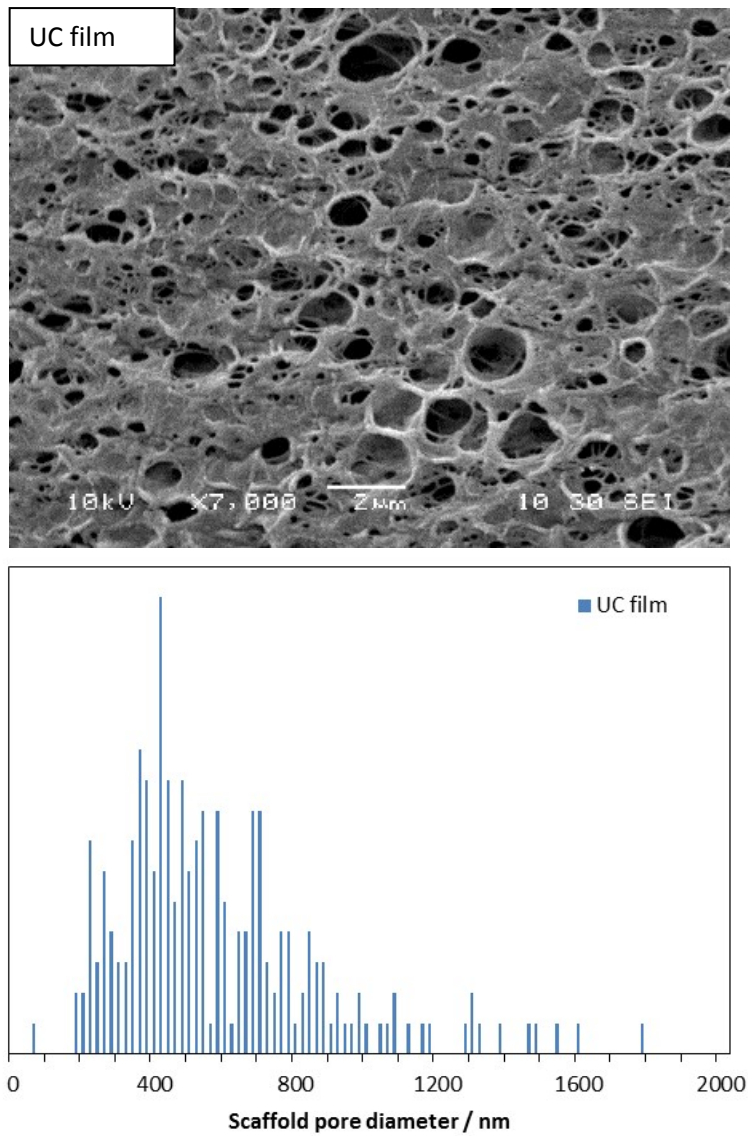


Fig. S19 SEM image of cast regenerated UC film (top). To determine the average pore size diameter SEM images were analysed using ImageJ software. Histogram of pore diameter for regenerated UC film (bottom).

Compressive load testing:

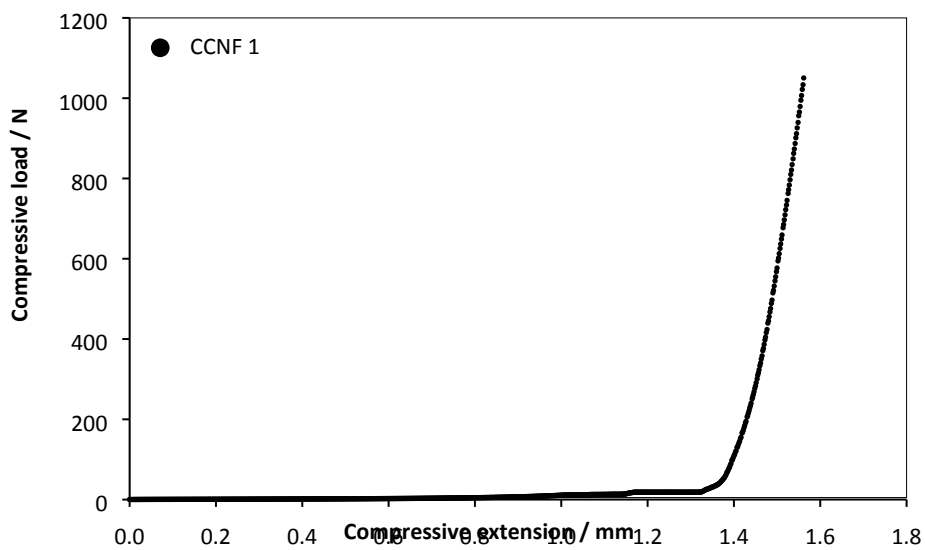


Fig. S20 CCNF lyophilised foam, compressive load vs. compressive extension graph, demonstrating the two phases of compression. The first phase represents the compression of the porous network, followed by the compressive load required to compress the bulk material.

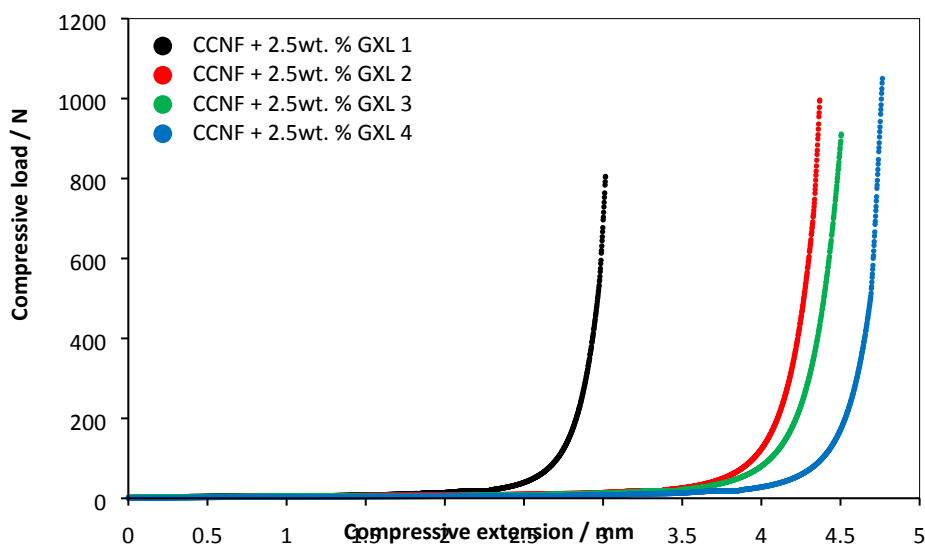


Fig. S21 CCNF + 2.5 wt. % glyoxal lyophilised foam, compressive load vs. compressive extension graph demonstrating the two phases of compression. The first phase represents the compression of the porous network, followed by the compressive load required to compress the bulk material.

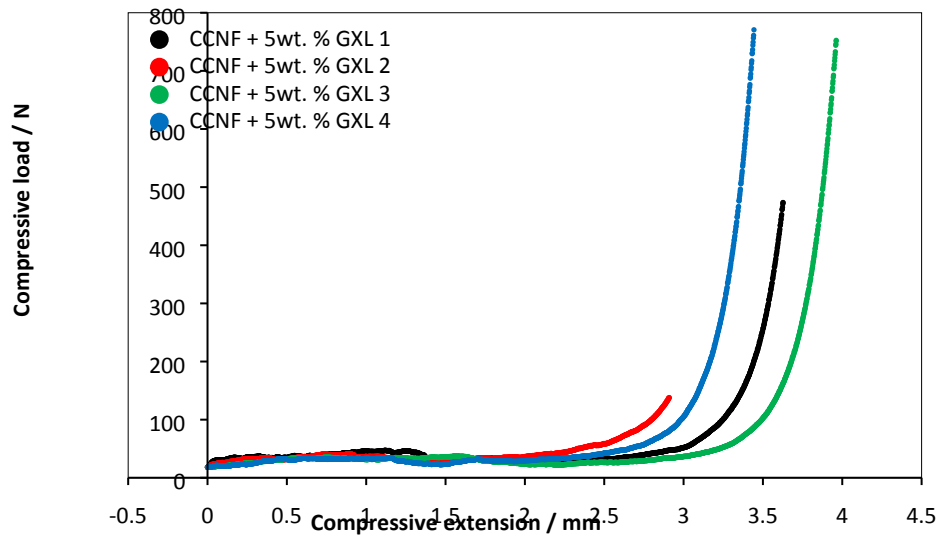


Fig. S22 CCNF + 5 wt. % glyoxal lyophilised foam, compressive load vs. compressive extension graph demonstrating the two phases of compression. The first phase represents the compression of the porous network, followed by the compressive load required to compress the bulk material.

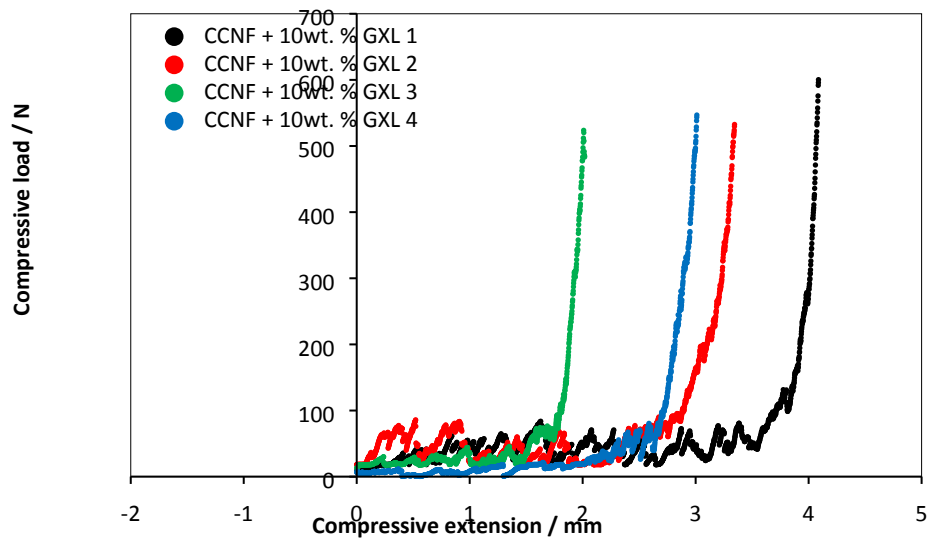


Fig. S23 CCNF + 10 wt. % glyoxal lyophilised foam, compressive load vs. compressive extension graph demonstrating the two phases of compression. The first phase represents the compression of the porous network, followed by the compressive load required to compress the bulk material.

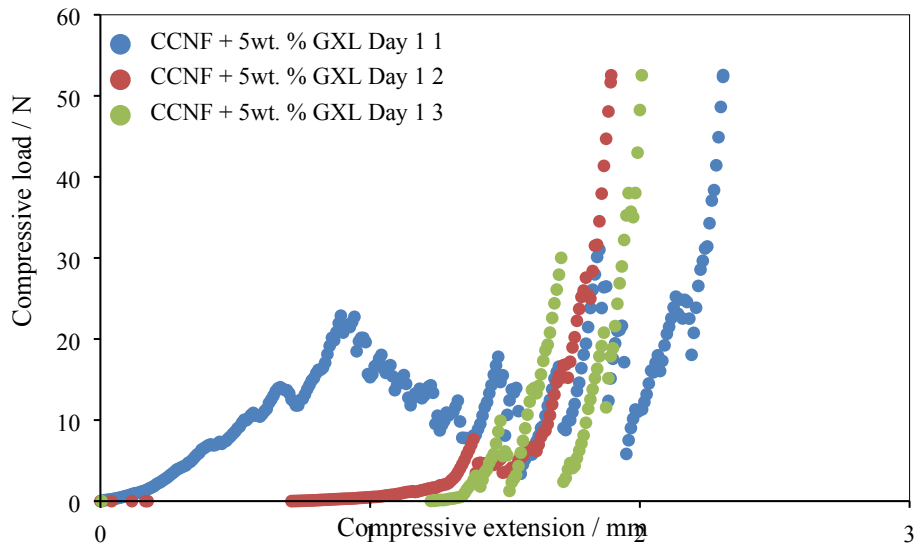


Fig. S24 CCNF + 5 wt. % glyoxal lyophilised foam, compressive load vs. compressive extension. Prior to testing samples were placed in PBS for 1 day to hydrate.

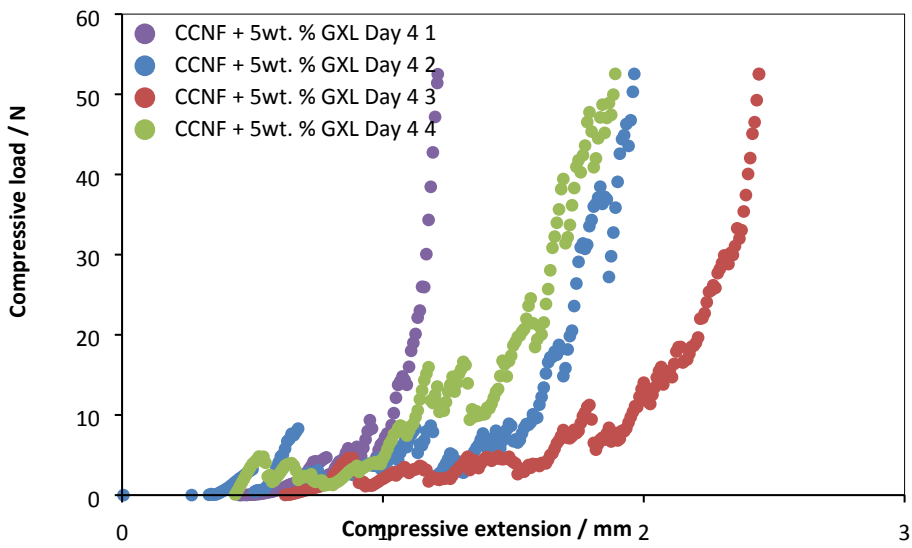


Fig. S25 CCNF + 5 wt. % glyoxal lyophilised foam, compressive load vs. compressive extension. Prior to testing samples were placed in PBS for 4 days to hydrate.

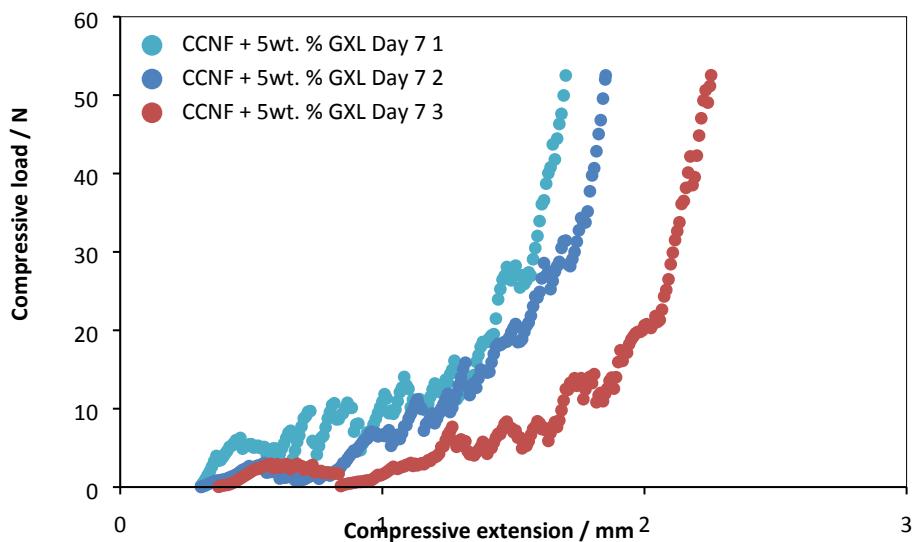


Fig. S26 CCNF + 5 wt. % glyoxal lyophilised foam, compressive load vs. compressive extension. Prior to testing samples were placed in PBS for 7 days to hydrate.

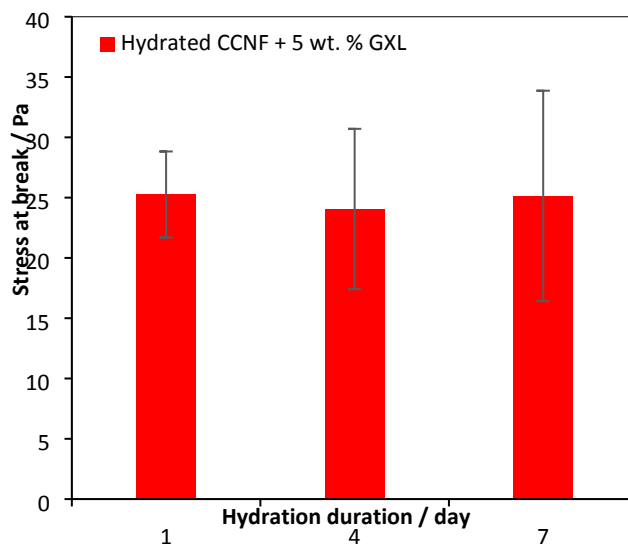


Fig. S27 Stress at break for samples of CCNF + 5 wt. % glyoxal lyophilised foam, hydrated for 1, 4 and 7 days prior to testing - stress calculated from the compressive load and cross sectional area of the sample. Hydrating the samples in PBS reduced the mechanical strength of the scaffolds, however, for CCNF XL foam (crosslinked with 5 wt. % glyoxal) there was no evidence of degradation of mechanical properties over 7 days. Conversely uncrosslinked CCNF foams collapsed to form hydrogels after only 1 day.

Cell visualisation:

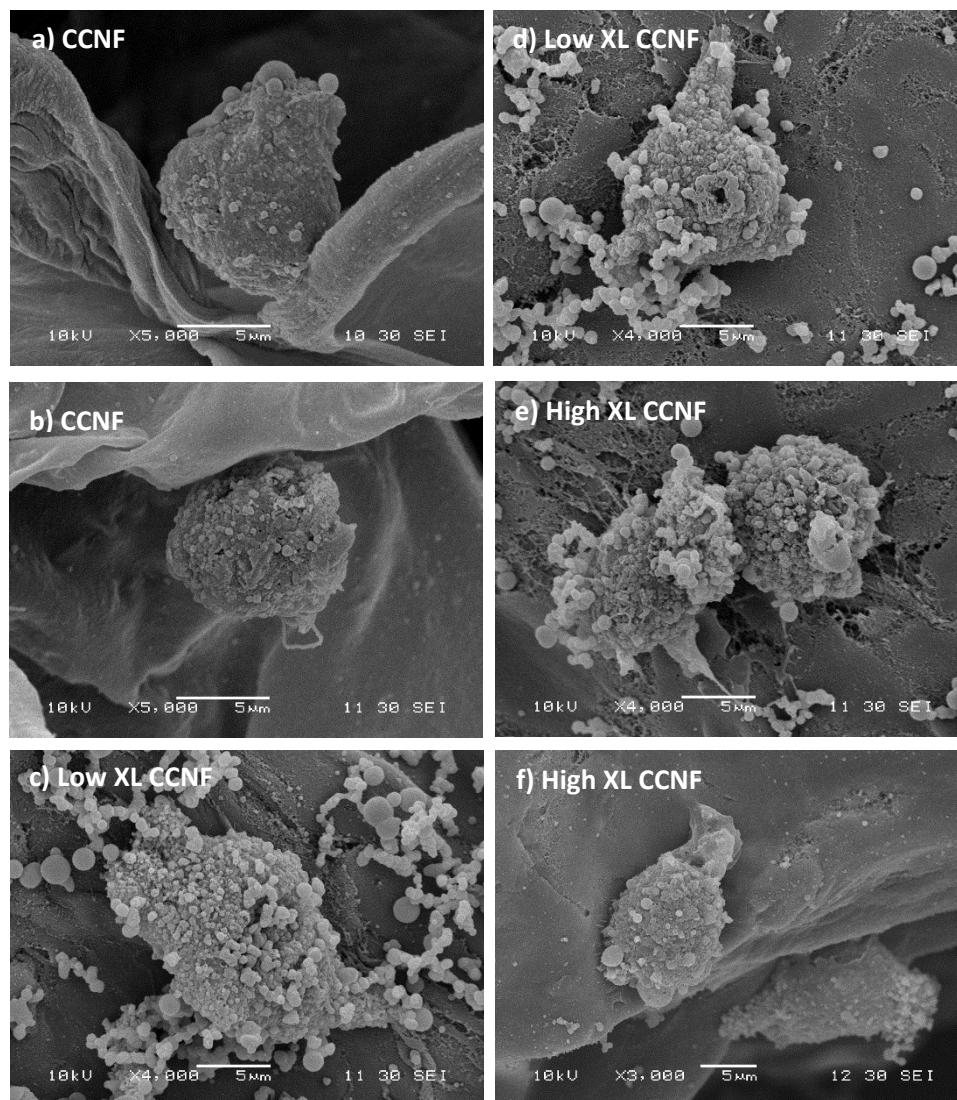


Fig. S28. SEM images of fixed MG-63 cells growing on the walls of 3D CCNF scaffolds. a-b) cationic cellulose c-d) Low XL cationic cellulose and e-f) High XL cationic cellulose, after 24 h incubation at 37 °C in 5 % CO₂. The attached cells appear to be more elongated on the XL cationic cellulose scaffolds, indicating spreading.

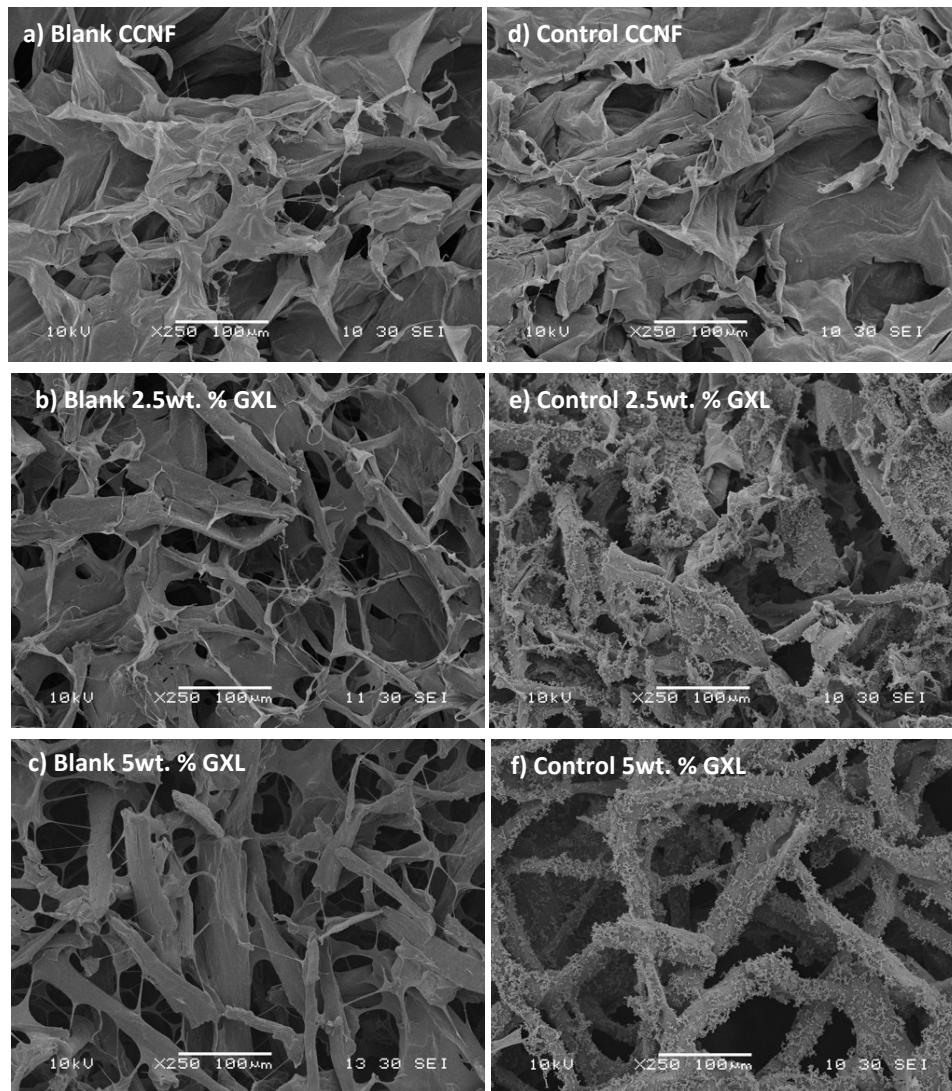


Fig. S29 SEM images of different lyophilised CCNF foams: a) – c) blank scaffolds, which were prepared using SEM following the methodology in the manuscript without being hydrated in cell culture media; d) – f) control scaffolds, which have been hydrated in FBS containing cell media without cells present. Some proteins within the media appear to be immobilised on the surface of XL CCNF scaffolds. The proteins could be fixed to the scaffold through the exposed aldehyde groups present in the XL surface.

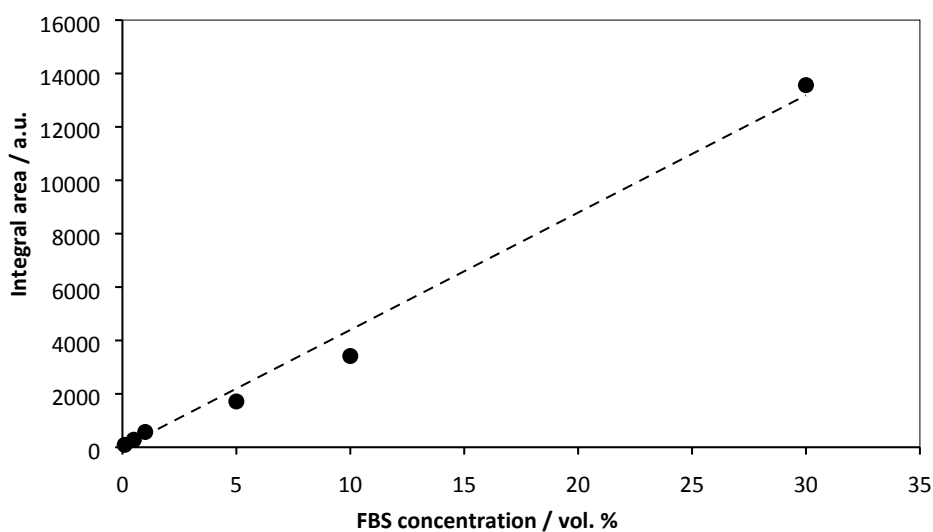


Fig. S30 FBS peak area for prepared standard solutions (0.1 – 30 vol. %). Calibration coefficient for glycolic acid was calculated from the gradient of the line to be 438.9 a.u./ vol. %. (n = 3, error bars = standard deviation)

References

1. J. C. Courtenay, M. A. Johns, F. Galembeck, C. Deneke, E. M. Lanzoni, C. A. Costa, J. L. Scott, and R. I. Sharma, *Cellulose*, 2017, **24**, 253–267.
2. M. Zaman, H. Xiao, F. Chibante, and Y. Ni, *Carbohydr. Polym.*, 2012, **89**, 163–70.
3. C. Schramm and B. Rinderer, *Anal. Chem.*, 2000, **72**, 5829–5833.
4. S. W. Provencher, *Comput. Phys. Commun.*, 1982, **27**, 213–227.
5. G. C. Borgia, R. J. S. Brown, and P. Fantazzini, *J. Magn. Reson.*, 2000, **147**, 273–285.
6. K. R. Brownstein and C. E. Tarr, *Phys. Rev. A*, 1979, **19**, 2446–2453.
7. D. Capitani, V. Di Tullio, and N. Proietti, *Prog. Nucl. Magn. Reson. Spectrosc.*, 2012, **64**, 29–69.